

Post-Repair Performance of Corroded Bond Critical RC Beams Repaired with CFRP

by B.C. Craig and K.A. Soudki

Synopsis: Presented in this paper is an investigation on the ability of externally applied fiber reinforced polymer (FRP) laminates to maintain bond of steel reinforcement in concrete members subjected to corrosion. Specimens were transversely confined with CFRP laminates in the bond zone after being subjected to various degrees of corrosion ranging from 2 to 10% theoretical mass loss. Some specimens were further corroded after repair to assess the effects of further structural deterioration. Control beams were subjected to minor amounts of corrosion and tested to failure without repair. Test results showed that CFRP wrapping was able to confine the corrosion cracking resulting in an overall flexural failure for all repaired specimens unlike the brittle bond splitting failures of the control specimens. CFRP confinement proved less effective at higher levels of pre-repair corrosion. Initial amounts of post-repair corrosion enhanced the performance of the CFRP repair by increasing the confining pressure; however the concrete rapidly deteriorated as the corrosion increased. In general, CFRP confinement was found to provide superior bond performance with respect to the unrepaired members indicating the potential future use in field applications of bond repair.

Keywords: bond; CFRP; confinement; corrosion; repair

564 Craig and Soudki

Brent C. Craig is a Civil Engineer within the Central Hydro Division at Acres International in Niagara Falls, Canada. He received his Master of Applied Science in Civil Engineering at the University of Waterloo in 2002. His graduate research focused on the use of externally applied fiber reinforced polymer laminates in the structural rehabilitation of concrete members.

Khaled Soudki is the Canada Research Chair Professor in Innovative Structural Rehabilitation at the University of Waterloo, Canada. He is a member of ACI Committees 440, Fiber Reinforced Polymer Reinforcement; 222, Corrosion of Metals; 546, Repair of Concrete; 550, Precast Concrete Structures. His research interests include corrosion, durability, rehabilitation, and strengthening of concrete structures using fiber reinforced polymer composites.

INTRODUCTION

The corrosion of steel reinforcement is a major concern in reinforced concrete (RC) infrastructure. Incidences of chloride-induced corrosion commonly lead to structural deficiencies and dangerous public safety concerns in highway bridges, parking garages, marine structures, and various other infrastructure. The option to replace structures is not always practical and performing repairs that are not durable may be costly to the owner and users. It is therefore important to find innovative methods to repair and/or strengthen deteriorated structures in an efficient, durable, and cost effective manner.

A primary influence of corrosion on the performance of flexural members is the degradation of bond interaction between the reinforcing steel and concrete, potentially resulting in catastrophic failures. Numerous studies have investigated the effects of corrosion on flexural members and shown that as the degree of corrosion increased, the loss of tensile steel area was not directly proportional to the loss in flexural capacity.^{1,2,3} At higher levels of corrosion, the loss of bond strength between the reinforcing steel and the concrete becomes more detrimental.^{1,2,3}

As stress levels increase in the tension reinforcement, bond forces radiate from the bar developing hoop stresses in the surrounding concrete.⁴ Bond forces are transferred from the steel to the concrete through chemical adhesion, friction and/or mechanical interlock.⁵ The interaction of each transfer mechanism depends on the configuration of the bar. However, the use of deformed bars allows mechanical interlock to be the most predominant form of transfer.⁵

Bond failure typically occurs in two distinct ways relating to the confinement of the reinforcing bar. In the presence of sufficient cover and or transverse reinforcement, a bond pullout failure is expected.⁶ In a bond pullout failure, concrete is able to withstand the radial tensile forces generated by the bond transfer force. However, failure is caused by localized shearing of the concrete between the reinforcing bar lugs, thus allowing the steel to pull through the concrete. When there is insufficient confinement, bond failure occurs when the tensile strength of the concrete is exceeded causing the development of

longitudinal cracks parallel to the reinforcing bar.^{7,8} Cracking causes a loss of confinement and mechanical interlock resulting in a bond splitting failure.

Corrosion of the reinforcing steel bar reduces the bond strength in several fashions. The development of corrosion products around the bar initially eliminates the chemical adhesion to the surrounding concrete. As corrosion progresses, frictional forces are reduced as the products may act as a lubricating layer.⁹ The expansive nature of the corrosion products develops hoop stresses in the surrounding concrete similar to those developed from bond forces. As the radial forces exceed the tensile capacity of the concrete, cracks develop resulting in a diminished mechanical interlock due to the reduced confining pressure. To a lesser degree, corrosion reduces steel rib cross section which has a negative impact of the mechanical interlock.⁹

It is important to note that low levels of corrosion have proven to be beneficial to bond forces.^{9,10,11} Prior to the tensile forces being exceeded in the concrete, the expansive pressure generated by the corrosion products increase the confining pressure around the bar, thus reducing slip potential. In addition, the initial formation of corrosion products increases the bar surface roughness and therefore increase the frictional component of the bond interaction.⁹

Confinement has a beneficial effect on the capacity of anchorage bond.^{12,13} By providing additional cover or transverse reinforcement, crack openings are minimized, thus better maintaining mechanical interlock. It still is important however to realize that inadequate development length could still lead to bond pullout failure regardless of the confinement provided.

Fiber reinforced polymer (FRP) reinforcement has emerged as viable solution to enhancing the bond capacity in existing RC members. FRP are light weight materials that provide excellent strength and durability. Literature has shown that the addition of externally applied FRP sheets does enhance the bond capacity in situations where adequate confinement is not provided.^{14,15,16,17,18}

To the author's knowledge, minimal research has been conducted on the potential use of FRP as a confining wrap in order to prevent the deterioration of bond in members subject to corrosive environments. The focus of this study is the investigation of the post-repair effects of FRP laminates on corrosion damaged, bond critical, RC members. Carbon FRP (CFRP) was used as a confining wrap in the bond zones to counteract the effects of corrosion and assist in maintaining mechanical interlock, thereby maintaining/enhancing the load carrying capabilities.

EXPERIMENTAL PROGRAM

The test program consisted of twenty-two medium-scale reinforced concrete bond-beam specimens. Beams were designed to investigate the effect of externally applied CFRP laminates with respect to maintaining the bond interaction between

566 Craig and Soudki

reinforcing steel and concrete in corrosion damaged flexural members. The test matrix for the study is provided in Table 1. Bond lengths were varied to examine the effectiveness of CFRP confinement for beams designed to fail either by flexure or bond. Bond lengths were controlled at 450 mm (series L1, $l_d/d_b = 28$), 350 mm (series L2, $l_d/d_b = 22$), and 250 mm (series L3, $l_d/d_b = 16$). Only series L3 with the 250 mm bond length was designed to fail by bond splitting in the uncorroded state.

To effectively investigate post-repair behavior, the specimens were subjected to initial degrees of corrosion prior to the application of the CFRP laminates. In some cases, specimens were further corroded to represent situations where the deterioration was not fully arrested. Four corrosion levels were selected to represent various degrees of deterioration (2, 5, 10 and 15% theoretical mass loss). Series L2, with the intermediate bond length of 350 mm, was corroded to the highest degree of post-repair corrosion to investigate section behavior at higher levels of mass loss. For each specified bond length, a control specimen was left uncorroded without any application of CFRP.

Specimen Design

The beam specimen measured 150 mm wide, 250 mm high and 2000 mm long as illustrated in Figure 1. Beams were reinforced to provide a ductile failure in the event that an adequate bond length was provided. Reinforcement consisted of two No. 15M, Grade 400, deformed bars to achieve a reinforcement ratio (ρ_s) of 0.012. The tension reinforcement was placed such that 25 mm of clear cover was maintained to the side and bottom of the bar ($c/d_b = 1.56$). The length of the reinforcing bar was selected such that a minimum of 100 mm was exposed on either end of the beam to allow for instrumentation. Shear zones were reinforced with 6 mm diameter stainless steel stirrups at 100 mm spacing to ensure adequate shear resistance. The 28-day concrete compressive strength was 42 MPa and the yield strength of the tension reinforcement was 440 MPa.

Reinforcing bars were debonded from the concrete outside of the bond zone using low-density polyethylene tube. Pockets were formed in the concrete tension zone near the midspan of the beam, outside of the bond zone, to allow for easy instrumentation of the tensile reinforcement during testing.

Induced Corrosion

Specimens were deteriorated using accelerated corrosion by means of an impressed current. The corrosion setup is shown in Figure 2. To facilitate the corrosion process, an 8 mm diameter hollow stainless steel tube was cast within the beam to act as an internal cathode. Furthermore, the concrete in the bottom third of the beam was contaminated with NaCl in order to produce a concrete mixture with 2.3% chlorides by mass of cement.

Specimens were connected in series by wires through the stainless steel bar and the tensile reinforcement to a power source. A constant current was applied such that the stainless steel bar acted as the cathode, and the tensile reinforcement as the anode in the corrosion reaction. The polyethylene debonding sleeves acted as insulator around the tension reinforcement ensuring that all corrosion occurred in the bond zones. Current

was applied in such a manner that the impressed current density of $105 \mu\text{A}/\text{cm}^2$ was maintained for all specimens.

Theoretical mass loss was calculated using Faradays Law, which specifies the amount of mass loss expected at a specific current density over a specific time frame (Jones, 1996). Specimens were corroded at room temperature in a humidity tent where they were subjected to cycles of 2.5 days at 100% relative humidity and 1 day dry for the duration of the corrosion period (Figure 2).

Wrapping Scheme

Deteriorated bond zones were confined using single unidirectional CFRP sheets. The CFRP sheets measured 0.11mm thick with a tensile strength of 2450 MPa, and an elastic modulus of 160 GPa. A single wrapping scheme was implemented for all bond regions as shown in Figure 1. CFRP laminates were transversely placed in the concrete-steel bond zone such that the fiber direction was oriented perpendicular to the direction of main reinforcement. Fiber sheets were fully wrapped around the beam to provide full confinement of the concrete section, thus preventing premature failure due to debonding of the CFRP sheet. It was assumed that in real world applications where CFRP sheets could not be wrapped around the entire beam, adequate anchorage or development length of the sheet would be applied through other means.

Test Setup

Specimens were tested to failure in four-point bending using the configuration shown in Figure 3. The specimens were simply supported over a span of 1800 mm, with a constant moment region measuring 300 mm.

Overall beam performance was monitored using a load cell and a displacement transducer (LVDT) located at the midspan of the beam. Slip displacement of the tensile steel was measured using LVDT's mounted to the free ends of the reinforcing bar. The LVDT's determined the free end slip by measuring relative displacement between the reinforcing steel and concrete surface as the bar was pulled through the concrete. The tensile steel stress was measured using 5 mm strain gauges attached to the bars within the pre-cast pockets at four locations.

Load was applied under displacement control at a rate of 1 mm/min until failure was achieved. Failure was considered to occur when concrete crushed in the compression zone (ultimate condition), or until the slip of the main reinforcing bar at one end reached a value of 10 mm (bond failure).

RESULTS AND DISCUSSION

A summary of test results is provided in Table 2. A significant difference in results could be observed for each bond length. For a complete understanding of the bond interaction, both the load-deflection and bond slip-stress curves must be examined. When calculating the bond stress, values from the strain gauges on the tension bars were

568 Craig and Soudki

used and averaged out over the length of the bar in order to simplify the analysis. When comparing specimens with different bond lengths, the bond stress is normalized by dividing the value by the ultimate theoretical bond stress for that particular bond length.

The actual mass loss values for the corroded reinforcing bar were determined after testing in accordance with ASTM G1-90. Results of the mass loss are provided in Table 2. For the purposes of analysis, the theoretical mass loss values are referred to in the text.

For all bond lengths, the control specimen failed by bond splitting action. For Series L1 and L2, this deviated from the designed mode of failure. The two percent theoretical mass loss provided enough loss of confinement to cause both specimens to fail abruptly. Series L1, with the longer bond length, was still able to achieve yielding of the reinforcing bar prior to loss of load carrying capabilities. Visually, the effect of the bond splitting is shown in Figure 4 where longitudinal cracks were developed along the length of the bar through the bond zone. These cracks were partially developed from existing corrosion cracks. Lack of confinement around the reinforcing bar is evident as the concrete is cracked and displaced in the bond region. At the time of failure, a sudden loss in load carrying capability for all three members can be seen in the form of an instantaneous drop on the load deflection curve (Figure 5). None of the members were able to achieve their full flexural capacity. Similar behavior may be observed for all beams with respect to their bond slip behavior (Figure 6). It is evident that the series with the longer bond length was able to develop bond stresses closer to the ultimate capacity. The following sections discuss the behaviour of the different test series.

Series L1– 450 mm Bond Length

Six beams were corroded and tested with a 450 mm bond length with five of the specimens subject to repair. Three beams were repaired at 2% mass loss with two beams being further corroded to 5 and 10% mass loss. The two remaining beams were repaired at 5% theoretical mass loss, with one beam being further corroded to 10% mass loss. The control beam was tested without repair after being subjected to 2% mass loss.

It is apparent from the load-deflection plots in Figure 7 that the post-repair beams were able to outperform the control beam. The repaired beams were able to achieve a ductile flexural failure. Analysis of the slip data indicated that unlike the control specimen, there was zero or negligible free end slip in the reinforcement for all repaired specimens. This indicates that none of the specimens provided any evidence of potential premature failure due to bond degradation. Therefore, for this series, the wrapping improved the performance of the corrosion damaged beams up to of 10% theoretical mass loss.

Series L2 – 350 mm Bond Length

This series incorporated ten beams to examine the post-repair behavior. Four beams were repaired at 2% mass loss with three being further corroded to 5, 10 and 15% mass loss. Three beams were repaired at 5% mass loss with two specimens further corroded to 10 and 15% mass loss. Two beams were repaired at 10% mass loss with one

further corroded to 15% mass loss. The remaining specimen acted as the control specimen and was tested without repair after being corroded to 2% mass loss.

Beams that were repaired at 2% theoretical mass loss were able to achieve a ductile flexural failure (Figure 8a). No additional deterioration was observed as the post-repair corrosion increased. Slip gauges indicate that little to no slip was measured up to failure of the specimen. At 10% mass loss, a slip of 0.04 mm was measured at the free end of only one bar indicating a potential weakening of the concrete around one of the tension bars. Slip initiation occurred around 3.66 MPa bond stress, which is 73% of the maximum predicted bond capacity. The slip was localized to one area of the tensile reinforcement and did not continue to propagate. The measurement is small and could be linked to experimental error. However, the possibility remains that under sustained load, the slip could continue eventually leading to failure. The high level of corrosion may have increased the confinement pressure beyond the compression strength of the concrete causing local crushing around the ribs leading to weakening of the bond strength. In general, the results indicate that beams in the L2 series confined at 2% mass loss were able to re-establish a ductile flexural failure with minimal indication of bond degradation. This result exhibits a significant improvement over the control specimen, which failed by bond splitting.

In terms of overall behavior, beams repaired at 5% mass loss show a similar trend to those repaired at 2% mass loss. Figure 8b shows that the load-deflection plots are relatively consistent with only slight differences most likely due to variations in material properties. However, when examining the local free end slip behaviour of the reinforcing bar, there is evidence that slip occurred in specimen W5C15, which was subjected to the highest level of post-repair corrosion. Specimen W5C10, corroded to 10% mass loss, behaved similarly to specimen W5C5 at 5% mass loss with little to no slip in the reinforcing bar at the time of failure. The additional post-repair corrosion damage induced in specimen W5C15 developed enough pressure to further deteriorate the concrete surrounding the reinforcement, thus weakening the mechanical interlock component of the bond. A free end slip of 0.07 mm was recorded at the time of failure. Slip initiation occurred at a bond stress of 3.60 MPa, which demonstrates a 28% reduction in bond stress at slip initiation relative to the theoretical maximum bond stress. This reduced level of bond stress at slip initiation is an indication of deterioration in the concrete, which could lead to a premature bond failure under sustained load conditions.

Specimens W10C10 and W10C15 exhibited load-deflection and load-slip behavior similar to the other flexural failures (Figure 8b). No significant degradation in bond strength was observed since no slip was recorded at the free ends of the tension steel. This indicates that specimen W10C10 out performed the other repaired beams corroded to 15 % mass loss (W2C15 and W5C15) due possibly to the initial bond enhancement created by small increases in the degree of corrosion. The concrete around the reinforcing bar was significantly cracked prior to repair, indicating that even though corrosion around the bar had occurred, some of the mechanical interlock could still be maintained. The small amount of corrosion after CFRP repair (2.2% experimental mass loss) has the potential of increasing the confining pressure in the bond zone since the

570 Craig and Soudki

expansion forces are restrained by the CFRP wrap. It is theorized that further increasing the post-repair corrosion levels would increase the internal pressure, locally exceeding the concrete strength around the reinforcing bar, and thus decreasing the bond strength.

Series L3 – 250 mm Bond Length

Similar to series L1, a total of six beams were examined in this series. Five beams were repaired at 2% and 5% mass loss with three beams being further corroded to higher levels up to 10% mass loss to examine the post-repair behavior. The sixth beam was tested without repair after attaining 2% mass loss.

Based on the load-deflection plot in Figure 9, the failure mode for all corroded and repaired specimens had a ductile flexural failure, whereas the control specimen was subjected to a brittle bond splitting failure. The overall load-deflection behavior of specimens W2C5, W2C10 and W5C10 was similar to the beams that were not subjected to any further corrosion after repair (W2C2 and W5C5). This shows that even after additional corrosion, the overall performance of the CFRP repaired specimens was superior to the control specimen, U2C2, which failed by bond splitting.

Examining the bond-slip curves, several observations can be made. The beams that were repaired at 2% mass loss had small amounts of free end slip at failure (Figure 10). The slip values of the steel reinforcing bar at failure were 0.06, 0.02, and 0.03 mm for specimens W2C2, W2C5 and W2C10, respectively. CFRP confinement to the concrete at the low corrosion levels preserved the integrity in the bond zone. Further corrosion after repair even up to high degrees of mass loss, up to 10%, did not damage the steel ribs and the surrounding concrete to a condition that would result in a bond failure. The internal pressure developed from the CFRP confinement allowed the reinforcing steel to continue to interact with the concrete. In turn, the added pressure reduced the overall slip by increasing the stiffness in the bond zone. Some degradation was observed at 10% mass loss with a 2% reduction in the slip initiation bond stress over the other two specimens. However, this change is very small and could be a result of other factors including experimental error.

Different results were observed for the beams repaired at 5% mass loss. When tested directly after wrapping, W5C5 exhibited a free end slip of 0.08 mm at failure. When the corrosion was continued after repair up to a mass loss of 10%, the slip value for specimen W5C10 significantly increased to 1.03 mm (Figure 11). The free-end slip at yield was 0.07 mm whereas specimen W5C5 had slip initiation after yielding of reinforcement bar. The bond stress at slip initiation for W5C10 was 7% lower than the ultimate bond stress, exhibiting noticeable degradation compared to other repaired specimens. The large increase in slip at ultimate denotes that a bond pullout failure was in progress. The residual bond force caused by friction due to confinement was sufficient to lead to a flexural failure under static load conditions. However, under sustained load or fatigue testing, a premature bond pullout failure would be expected.

Effect of Bond Length

In general, the overall effect of the confinement on the bond strength was similar for all bond lengths. The repaired specimens outperformed the control specimens as their failure mode was effectively altered from a bond splitting failure to a more ductile flexural failure. Similarly, regardless of bond length, all members were able to achieve the full bond stress.

It was found that when the initial bond length was adequate, confinement at low degrees of corrosion was able to reinstate the full flexural capacity of the members. Where specimens were designed with inadequate bond lengths, FRP confinement was limited to preventing bond splitting failures.

The importance of sufficient bond length is evident when examining the free end slip and the slip initiation bond stress. In the cases of ample bond length, reinforcing bars maintained bond behavior in the concrete up to high levels of corrosion. The L2 series showed slight potential for bond pullout failures at corrosion levels of 15% mass loss. In the case of the bond-deficient length (series L3), significant bond slip was evident in most post-repair conditions. This was more evident when confinement was applied after significant pre-repair corrosion had occurred.

In summary, post repair analysis shows that the application of the CFRP wrap must be implemented prior to excessive damage of the concrete.

CONCLUSION

Post-repair performance testing demonstrated the confining ability of CFRP wrap. CFRP repair may lead to higher bond strengths but under conditions of increased corrosion after repair, bond failure is still possible in the form of a pullout failure as opposed to the bond splitting failure witnessed in the unconfined corroded specimens. Corrosion plays a devastating role in reducing the structural capacity of unconfined flexural members. CFRP confinement of the bond zone in bond-beam specimens serves to maintain steel-concrete bond interaction. CFRP resisted the expansion forces caused by corrosion, thus reducing crack growth and maintaining the interlock between the reinforcing steel and concrete. As post-repair corrosion progressed, cracks were unable to expand due to the presence of CFRP sheets. In turn, CFRP developed stresses, which increased the internal confining pressure around the reinforcing bar that counteracted the expansion stresses due to corrosion.

The effect of CFRP on the confinement of corrosion-damaged members varies depending on whether the member has adequate bond or is bond deficient. For those members with inadequate bond length, the added CFRP confinement improved the performance of bond-deficient corroded members allowing them to outperform the unconfined specimen. It is important to understand the nature of failure of the CFRP confined specimens. Since no cracks were visible with the CFRP wrap in place, there are no indications of failures. Even under conditions of high ultimate bond stresses, the

572 Craig and Soudki

presence of low slip initiation bond stresses indicates that failure could potentially occur prematurely by bond pullout in the case of sustained loading or creep.

Confinement was found to be more effective when applied prior to excessive corrosion of the specimens. Typically, small amounts of post-repair corrosion were found to have no effect or in some instances helped increase bond strength as a result of increased confining pressures. However, as the post-repair corrosion levels increased, the bond strength deteriorated.

The overall structural performance of beams wrapped with CFRP was enhanced. However, caution and engineering judgement must be used in the application of this repair method since abrupt failure of the member due to bond pullout failure could occur without warning if repair is performed at high corrosion levels or if members were initially designed with inadequate bond. The confining wrap may increase the bond strength, but as with all repairs, this should not be used as a band-aid solution, and the cause of deterioration must be addressed to prevent further corrosion and deterioration.

ACKNOWLEDGEMENTS

This research is conducted with financial assistance from ISIS Canada Network of Centres of Excellence and Natural Sciences and Engineering Research Council of Canada.

REFERENCES

1. Uomoto, T., Tsuji, K., and Kakizawa, T. (1984) "Deterioration Mechanism of Concrete Structures Caused by Corrosion of Reinforcing Bars," Transaction of the Japan Concrete Institute, Vol. 6. pp. 163-170.
2. Capozucca, R. (1995) "Damage to Reinforced Concrete due to Reinforcement Corrosion," Construction and Building Materials, Vol. 9, No. 5, pp. 295-303.
3. Mangat, P.S. and Elgarf, M.S. (1999) "Flexural Strength of Concrete Beams with Corroding Reinforcement," ACI Structural Journal, Vol. 96, No. 1, pp. 149-158.
4. Tepfers, R. (1979) "Cracking of Concrete Cover along Anchored Deformed Reinforcing Bars," Magazine of Concrete Research, Vol. 31, No. 106, pp. 3-12.
5. Lutz, L.A. and Gergely, P. (1967) "Mechanics of Bond and Slip of Deformed Bars in Concrete," ACI Journal, Vol. 64, No. 11, pp. 711-721.
6. Cairns, J. and Abdullah, R.B. (1996) "Bond Strength of Black and Epoxy-Coated Reinforcement – A Theoretical Approach," ACI Materials Journal, Vol. 93, No. 4, pp. 362-369.
7. Ferguson, P.M. (1966) "Bond Stress – The State of the Art," ACI Committee 408, Journal of the American Concrete Institute, November, pp. 1161-1180.

8. Pillai, S.U., Kirk, D.W., and Erki, M.A. (1999) "Reinforced Concrete Design: Third Edition," McGraw-Hill Ryerson Limited, Ontario, Canada.
9. Almusallam, A.A., Al-Gahtani, A.S., Aziz, A.R., and Rasheeduzzafar (1996) "Effect of Reinforcement Corrosion on Bond Strength," *Construction and Building Materials*, Vol. 10, No. 2, pp. 123-129.
10. Al-Sulaimani, G.J., Kaleemullah, M., Basunbul, I.A., and Rasheeduzzafar (1990) "Influence of Corrosion and Cracking on Bond Behavior and Strength of Reinforced Concrete Members," *ACI Structural Journal*, Vol. 87, No. 2, pp. 220-231.
11. Cabrera, J.G. (1996) "Deterioration of Concrete due to Reinforcement Steel Corrosion," *Cement & Concrete Composites*, Vol. 18, pp. 47-59.
12. Soroushian, P., Choi, K., Park, G., Aslani, F., (1991) "Bond of Deformed Bars to Concrete: Effects of Confinement and Strength of Concrete," *ACI Materials Journal*, Vol. 88, No. 3, pp. 227-232.
13. Giuriani, E. and Plizzari, G.A. (1998) "Confinement Role in Anchorage Capacity," *American Concrete Institute SP-180*, MI, USA, pp. 171-193.
14. Kono, S., Inazumi, M., And Kaku, T. (1998) "Evaluation of Confining Effects of CFRP Sheets on Reinforced Concrete Members," *Proceedings: Second International Conference on Composites in Infrastructure*, Tucson, AZ, pp. 343-355.
15. Hamad, B.S., Soudki, K.A., (2001) "GFRP Wraps for Confinement of Bond Critical Regions in Beams," *Proceedings: Composites in Construction International Conference*, 10-12 October, Porto, Portugal.
16. Hamad, B., Rteil, A., Selwan, B., Soudki, K.A. (2004) "Behavior of Bond Critical Regions Wrapped with FRP Sheets in Normal and High Strength Concrete," *ASCE Journal of Composites for Construction*, Vol. 8, No. 3, 248-257.
17. Hamad, B., Rteil, A., Soudki, K.A., 2004. "Tension Lap Splices in High-Strength Concrete Beams Strengthened with GFRP Wraps," *ASCE Journal of Composites for Construction*, Vol. 8, No. 1, pp. 14-21.
18. Soudki, K.A. and Sherwood, E.G., (2003) "Bond Behaviour of Corroded Steel Reinforcement in Concrete Wrapped with Carbon Fibre Reinforced Polymer Sheets," *ASCE Journal of Materials in Civil Engineering*, Vol. 15, No. 4, pp. 358-370.

Table 1 – Experimental Test Matrix

Strengthening Scheme	Theoretical Degree of Corrosion (% mass loss)			
	2	5	10	15
Unconfined	U2C2			
Wrapped @ 2%	W2C2	W2C5	W2C10	W2C15*
Wrapped @ 5%		W5C5	W5C10	W5C15*
Wrapped @ 10%			W10C10*	W10C15*

* Specimens apply to series L2 only

Table 2 – Experimental Test Results

Specimen	Experimental Mass Loss (%)	Failure				Slip Initiation Bond Stress (MPa)
		Mode	Load (kN)	Bond Stress (MPa)	Slip (mm)	
Series L1 - 450 mm Bond Length						
U2C2	4.0	Bond Splitting	87.5	3.91	0.24	3.66
W2C2	4.5	Flexure	96.4	3.91	0.01	N/A
W2C5	6.0	Flexure	96.1	3.89	0.00	N/A
W2C10	7.2	Flexure	98.6	3.76	0.00	N/A
W5C5	6.7	Flexure	98.5	3.91	0.00	N/A
W5C10	10.2	Flexure	98.1	3.91	0.00	N/A
Series L2 - 350 mm Bond Length						
U2C2	3.2	Bond Splitting	87.9	4.99	0.13	3.96
W2C2	4.4	Flexure	94.1	5.03	0.01	N/A
W2C5	5.7	Flexure	106.9	5.03	0.00	N/A
W2C10	8.5	Flexure	98.7	4.89	0.03	3.66
W2C15	10.3	Flexure	97.1	5.03	0.01	N/A
W5C5	7.6	Flexure	98.7	5.03	0.03	4.19
W5C10	8.5	Flexure	96.5	4.97	0.00	N/A
W5C15	11.5	Flexure	96.2	5.03	0.07	3.6
W10C10	10.4	Flexure	96.6	5.03	0.01	N/A
W10C15	11.6	Flexure	97.2	5.03	0.01	N/A
Series L3 - 250 mm Bond Length						
U2C2	3.6	Bond Splitting	65	5.53	0.16	4.48
W2C2	4.6	Flexure	94.5	7.04	0.06	7.04
W2C5	6.5	Flexure	94.8	7.04	0.02	7.04
W2C10	8.2	Flexure	97.8	7.04	0.03	6.9
W5C5	7.4	Flexure	98.4	7.04	0.08	7.04
W5C10	11.5	Flexure	103.5	7.04	1.03	6.56

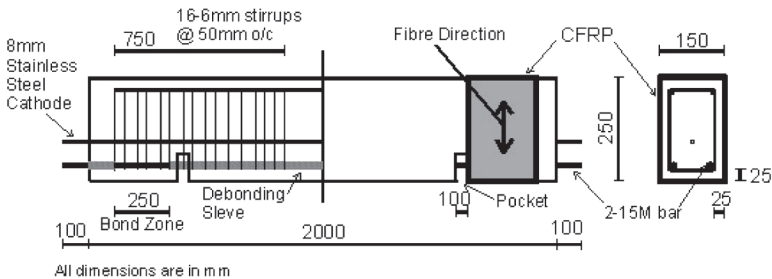


Figure 1 – Test Specimen Reinforcement and CFRP Layout

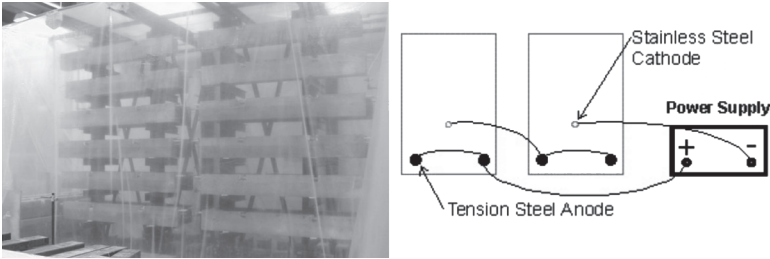


Figure 2 – Corrosion Tent and Electrical Setup

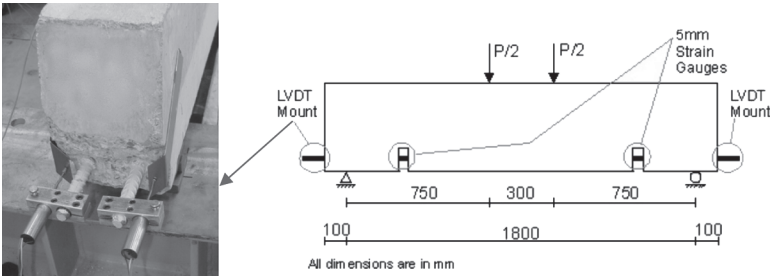


Figure 3 – Test Setup and Instrumentation



Figure 4 – Bond Splitting Failure Crack Pattern, Series L1

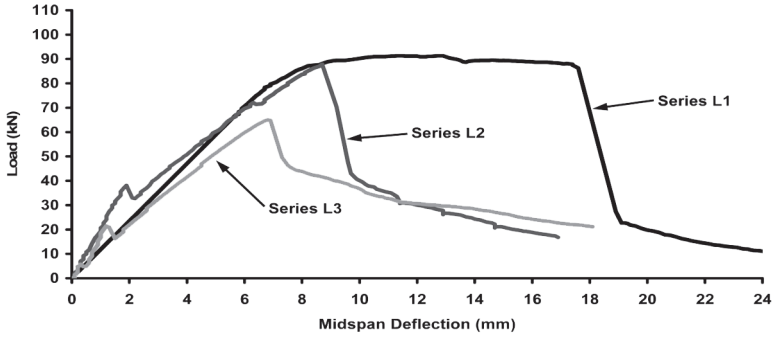


Figure 5 – Load-Deflection Curve for Unconfined Members

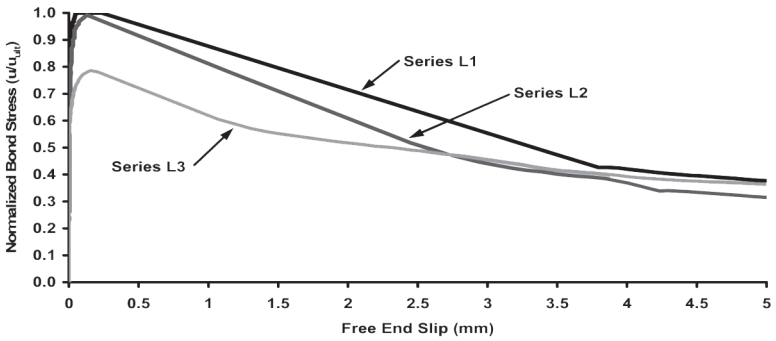


Figure 6 – Bond Stress vs. Free End Slip for Unconfined Members

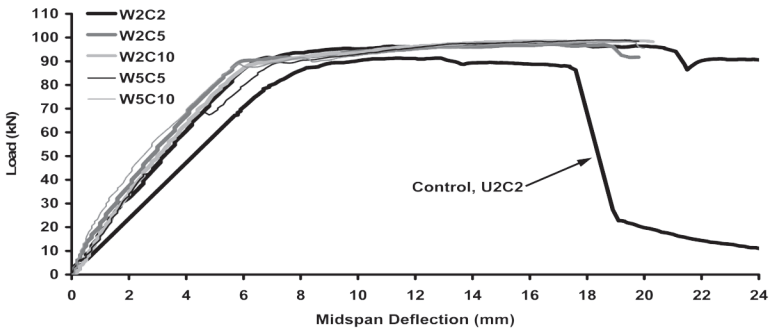


Figure 7 – Load-Deflection Behavior, Series L1

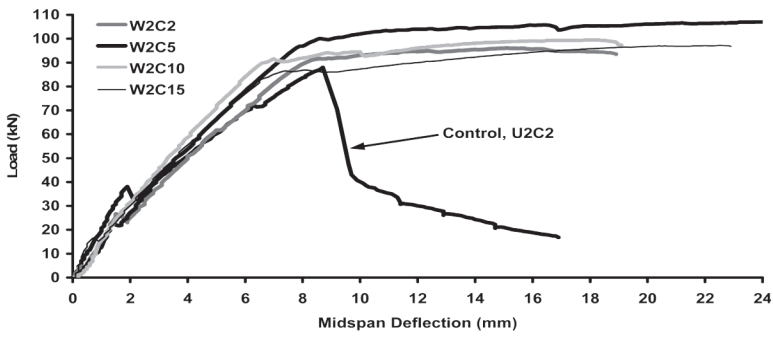


Figure 8a – Load-Deflection Behavior, Series L2

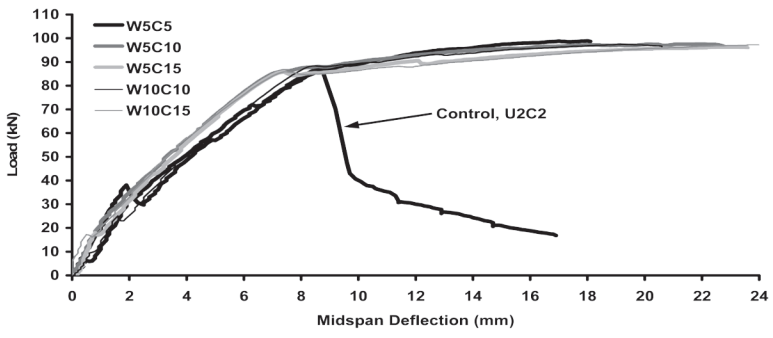


Figure 8b – Load-Deflection Behavior, Series L2

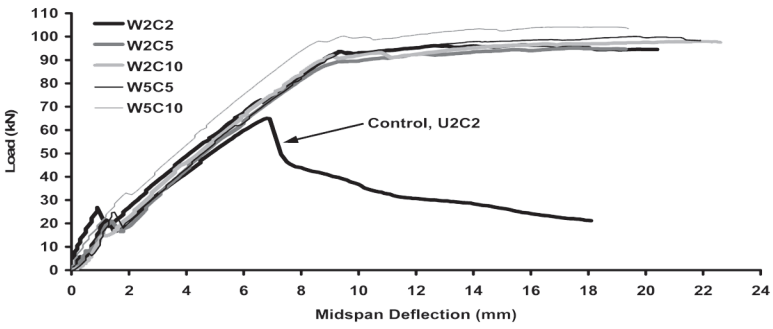


Figure 9 – Load-Deflection Behavior, Series L3

578 Craig and Soudki

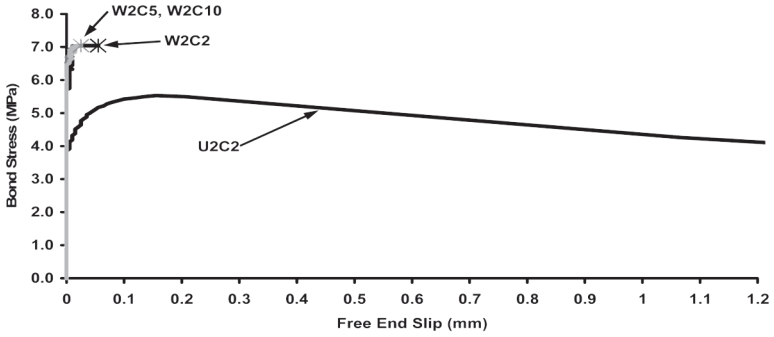


Figure 10 – Bond Slip Behavior, Series L3, Repaired at 2% Mass Loss

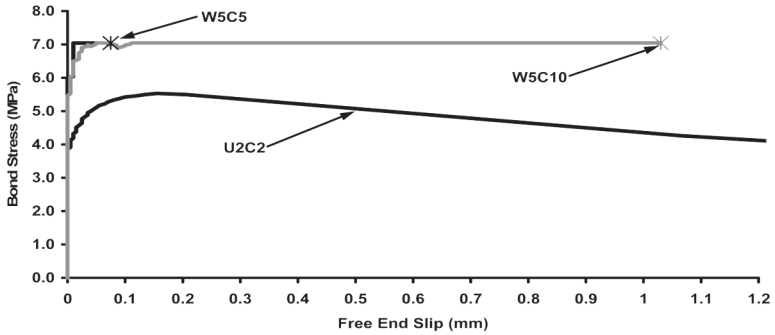


Figure 11 – Bond Slip Behavior, Series L3, Repaired at 5% Mass Loss